Transactions on the Built Environment vol 29, © 1997 WIT Press, www.witpress.com, ISSN 1743-3509

DEVELOPMENT OF A SYSTEM FOR THE ESTIMATION OF FRFs USING MIMO TECHNIQUE

Ricardo F. M. de Andrade, Carlos Magluta and Ney Roitman
COPPE/UFRJ - Civil Engineering Department
E-mail: andrade@labest.coc.ufrj.br

Abstract -- The present paper treats with the development of a system for estimating the Frequency Response Functions (FRFs) using Multiple Input Multiple Output (MIMO) Technique. The system was developed using LabVIEW software (Laboratory Virtual Instrument Engineering Workbench), which uses a graphical programming language, and includes libraries for data acquisition, instrument control, data analysis and data presentation. Results of experimental tests carried on a prototype of a simply supported beam were used to test the developed system. Experimental tests were also carried on a small scale model of an offshore platform using two orthogonal simultaneous random excitations. The response of 32 accelerometers were measured, and the obtained FRFs between all acceleration responses and excitation forces were calculated. The obtained FRFs were then used to estimate the modal parameters. According to the tests, the developed system could be used for experimental tests of small scale models and offshore structures prototypes.

NOMENCLATURE

FRF - frequency response function
G_{iy} - crosspower spectra of the i^{th} input force and the output
G_{nn} - autopower spectrum of the noise of the system
G_{q1} - crosspower spectrum of the input forces
$[G_{xx}]$ - matrix of the auto- and crosspower spectra of the input forces
$[G_{xxy}]$ - augmented spectral matrix
G_{yy} - autopower spectra of the output

$G_{yy.q!}$ - conditioned autopower spectra of the output
H_{iy} - FRF of the i^{th} input and the output
H_1 - least squares estimator
H_V - total least squares estimator
$m_i(t)$ - time signal of the noise in the i^{th} input force
$M_i(f)$ - noise in the i^{th} input force in the frequency domain
$n(t)$ - time signal of the noise in the output $y(t)$
$N(f)$ - noise in the output in the frequency domain
q - number of input forces
$[V]$ - eigenvectors matrix
$x_i(t)$ - time signal of the i^{th} input force
$X_i(f)$ - i^{th} input force in the frequency domain
$y(t)$ - time signal of the acceleration output due to all input forces
$Y(f)$ - acceleration output in the frequency domain
$y_i(t)$ - time signal of the acceleration output due to the i^{th} input force
γ^2 - multiple coherence function
λ_i - eigenvalue
$[\Lambda]$ - eigenvalues diagonal matrix

INTRODUCTION

Modal analysis[1-4] is a series of techniques that aims to describe the behavior of structures based on the relationship between their excitations and responses. The accurate estimation of the FRFs is of prime importance, since the modal parameters, i.e., the natural frequencies, damping factors and modal vectors, depend directly from the estimated FRFs.

The Multiple Input Multiple Output (MIMO) technique has been lately used for the estimation of the FRFs. It shows many potential advantages[3] over the Single Input Multiple Output (SIMO) technique, such as: (i) the increase of the accuracy of the estimates; (ii) the evenly distribution of the excitation energy, which decreases the effects of local non-linearities; (iii) the consistency of the data taken simultaneously, which decreases errors due to time-dependent system characteristics, changing boundary conditions and other experimental considerations.

The consistency between rows and columns of the FRF matrix has become very important, since many parameter estimation algorithms use multiple measurements for the estimation of modal parameters, like the orthogonal polynomial method[5].

Transactions on the Built Environment vol 29, © 1997 WIT Press, www.witpress.com, ISSN 1743-3509

The developed system presented in this paper uses the Least Squares technique (H_1) and the Total Least Squares technique (H_V) for estimating the FRFs of structures. In the preliminary tests, the FRFs obtained with the system were compared with the results obtained using a current use Spectrum Analyzer. The system was then used for experimental tests in a complex structure, in order to evaluate the efficiency of multiple excitation.

MULTIPLE INPUT MULTIPLE OUTPUT (MIMO) THEORY

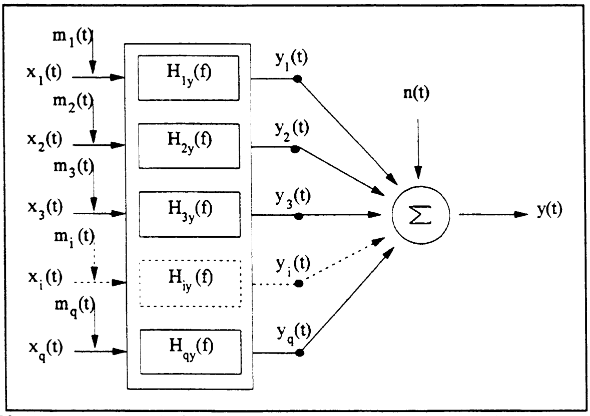

Figure 1 - Multiple Input Single Output (MISO) System

Figure 1 shows the general Multiple Input Single Output (MISO) model for **q** inputs and one output, where the terms $x_i(t), i = 1,2,\ldots,q$ represent the measured input records and $y(t)$, the measured output record. The noises of the system are represented by $m_i(t)$ and $n(t)$. In order to obtain a MIMO[3,6] model, it is necessary to consider any other output response of the system, but the input forces remain always the same. Equation 1 describes the system of Figure 1 in the frequency domain, which can be written as:

$$Y(f) + N(f) = \sum_{i=1}^{q} H_{iy}(f)\left(X_i(f) + M_i(f)\right) \qquad (1)$$

Least Squares Estimator - H_1

Assuming that there are no measurement errors on the input forces ($M_i(f)=0$), the H_1 least squares technique[6-8] aims at finding the solution of Equation 1 that minimizes the error N(f). After some mathematical development, one can obtain the FRF estimator H_1 written in terms of the auto- and crosspower spectra of input forces and the response signal, as it can be seen in Equation (2):

$$\begin{bmatrix} G_{11} & \cdots & G_{1q} \\ \vdots & & \vdots \\ G_{q1} & \cdots & G_{qq} \end{bmatrix} \begin{Bmatrix} H_{1y} \\ \vdots \\ H_{qy} \end{Bmatrix} = \begin{Bmatrix} G_{1y} \\ \vdots \\ G_{qy} \end{Bmatrix} \tag{2}$$

where $G_{qy}(f) = \sum X_q^*(f)\,Y(f)$ is the crosspower spectra of the input force $X_q(f)$ and the response $Y(f)$, obtained by applying a fast Fourier transform upon the time signal.

The solution of the set of simultaneous equations with the FRFs as the unknowns described in Equation (2) can be obtained using the Gauss elimination procedure[3,6] applied on the augmented spectral matrix $\left[G_{xxy}\right]$, defined in Equation (3), in order to compute also the multiple coherence:

$$\left[G_{xxy}\right] = \begin{bmatrix} G_{11} & \cdots & G_{1q} & G_{1y} \\ \vdots & & \vdots & \vdots \\ G_{q1} & \cdots & G_{qq} & G_{qy} \\ G_{y1} & G_{y2} & G_{yq} & G_{yy} \end{bmatrix} \tag{3}$$

It should be noted that the solution presented in Equation (3) is only for one response, and should be repeated for all discrete frequencies of the analysis. For any other response, only the last row and column must be updated. The matrix $\left[G_{xx}\right]$ however is the same for all responses, and does not need to be recalculated. In order to exist a solution for the problem, the matrix of the auto- and crosspower spectra of the input forces $\left[G_{xx}\right]$ must not be singular. The results are obtained in the form of the matrix presented in Equation (4), where it can be seen that the FRFs can be found through backsubstitution using the conditioned equations. The conditioned equations are obtained by taking off the influence of one row over the others.

$$\begin{bmatrix} G_{11} & \cdots & G_{1q} & G_{1y} \\ \vdots & & \vdots & \vdots \\ 0 & \cdots & G_{qq.(q-1)!} & G_{qy.(q-1)!} \\ 0 & \cdots & 0 & G_{yy.q!} \end{bmatrix} \tag{4}$$

The single term of the last row is the amount of the error of the system, since it represents the response of the system due to none of the previous input forces. The multiple coherence, which represents the relationship between the response and all known excitations, can be written as Equation (5):

$$\gamma^2 = 1 - \frac{G_{yy.q!}}{G_{yy}} \tag{5}$$

Total Least Squares Estimator - H_V

Assuming now measurement errors on both input forces and response signal, represented by $M_i(f)$ and $N(f)$, the H_V total least squares technique[3,7,8] aims at finding the solution that minimize the sum of both squared errors. It is proved in the literature[7] that it can be achieved by applying the eigenvalue decomposition upon the augmented spectral matrix, defined in Equation (3). The matrix $\left[G_{xxy}\right]$ is hermitian, therefore the eigenvalue can be defined by Equation (6):

$$\left[G_{xxy}\right] = [V][\Lambda][V]^h \tag{6}$$

where $[\Lambda] = \text{diag}\left(\lambda_1, \lambda_2, \ldots, \lambda_{q+1}\right)$ are the eigenvalues, and $[V]^h[V] = I$, where $[V]$ are the eigenvectors. The total least squares estimate H_V is then defined by Equation (7):

$$\{H_v\} = \begin{Bmatrix} -\dfrac{V_{1\,q+1}}{V_{q+1\,q+1}} \\ \vdots \\ -\dfrac{V_{q\,q+1}}{V_{q+1\,q+1}} \end{Bmatrix} \tag{7}$$

It must be noted that the solution does not exist if $V_{q+1\,q+1} = 0$. This however can only happen if the submatrix $\left[G_{xx}\right]$ from matrix $\left[G_{xxy}\right]$ is singular, that is, if the input forces are linear dependent. Verifying that the input forces are not totally correlated with each other is therefore sufficient to warrant the existence of the solution.

The magnitude of the errors on the response signal can be expressed by Equation (8) and the multiple coherence is defined in Equation (9).

$$G_{nn} = \lambda_{q+1} V^*_{q+1\,q+1} V_{q+1\,q+1}. \tag{8}$$

$$\gamma^2 = 1 - \frac{G_{nn}}{G_{yy}} \tag{9}$$

A comparison of least squares (H_1) and total least squares (H_V) technique can be better explained[3] by analyzing Figure 2. The H_1 technique aims at minimizing the errors only in the direction of the output response (y-axis). The H_V technique aims at minimizing the errors in both input and output response direction, in such a manner that the perpendicular distances are considered.

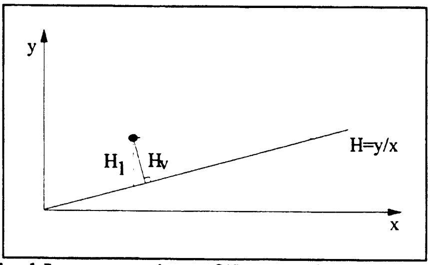

Figure 2 - Geometrical Interpretation of Error Minimization Technique H_1 and H_V.

SYSTEM IMPLEMENTATION

The system was implemented using LabVIEW software[9] (Laboratory Virtual Instrument Engineering Workbench), which is a program development application that uses a graphical programming language, G, to create programs in a block diagram form. LabVIEW includes libraries for data acquisition, GPIB and serial instrument control, data analysis, data presentation, and data storage.

The implemented system consists of three main blocks:

- **System Configuration** - In this initial block, which must be accessed before all the others, the main data of the analysis must be defined, including the hardware, the table with calibration constants, position and direction of all sensors, and of the excitation forces. It allows also a visual inspection of all time signals to be acquired.

- **Data Processing** - In this second block, the FRFs estimates will be calculated. All the process is based on the spectral matrix defined in Equation (3). The system acquires all time signals, processes the FFTs (fast Fourier transform) of the signals, calculates the auto- and crosspower spectra between all signals, and calculates the FRFs estimates for the H_1 and

H_V estimators. In this block, two graphs chosen by the user can be displayed to allow the observation of the FRFs estimates with the increasing number of samples. Analyzing the coherence functions or with visual inspection of the estimates, the user decides if the estimates are already good. A typical screen of the data processing can be seen in Figure 3.

- **Data Storing** - In the last block, the calculated data will the stored. In order to allow a real-time acquisition, all the desired data will be calculated just before they will be stored. The processing is therefore faster, since only two graphs and the spectral matrix are calculated in the data processing block. The desired results are then stored in a Universal File Format (UFF), which will be used in parameter estimation methods to obtain the natural frequencies, damping and mode shapes of the tested structure.

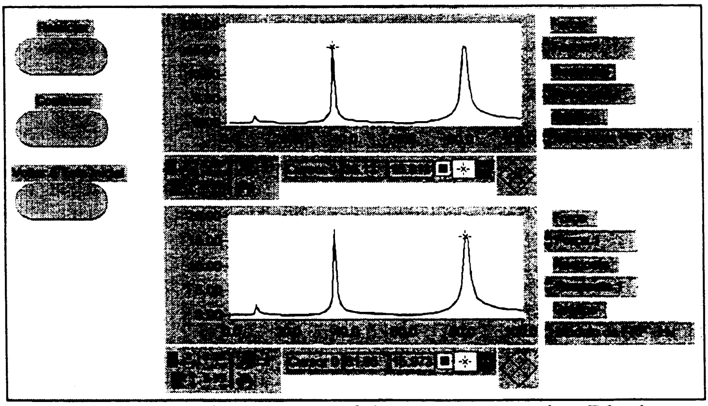

Figure 3 - Typical Screen of the Data Processing Block.

PRELIMINARY TESTS

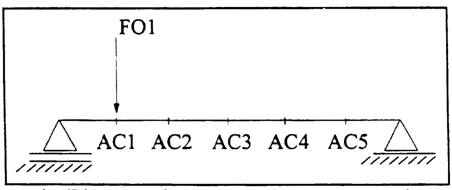

Figure 4 - Schematic Figure of the Simply Supported Beam Used for the Preliminary Tests of the System.

In order to test the developed system, experimental tests were carried on a simply supported beam, showed schematically in Figure 4. The results obtained with the utilization of the system for the H_1 estimator were compared with results obtained simultaneously with a current use spectrum analyzer. The comparison of a typical FRF estimate of the accelerance of the force FO1 and the response measured in AC1 can be seen in Figure 5, where it can be noted the good agreement of the results obtained with the implemented system and with the spectrum analyzer.

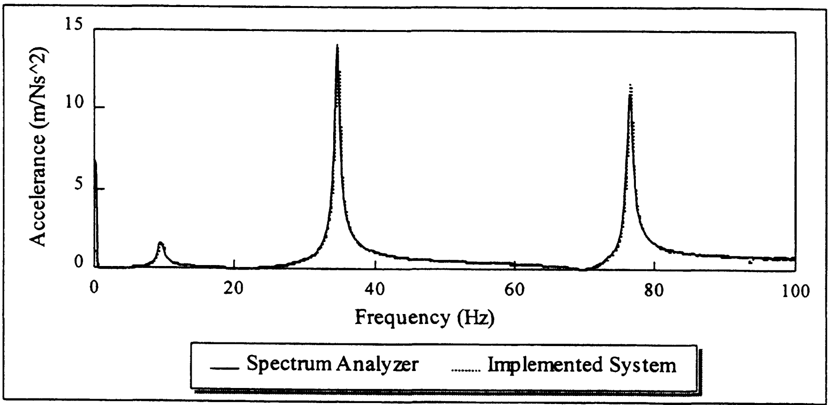

Figure 5 - Comparison of the H_1 estimates obtained simultaneously with the implemented system and a current use spectrum analyzer.

Little differences were observed between the FRFs obtained with the H_1 and H_V estimators. Figure 6 shows a comparison of the estimates for random input force applied and measured in AC1, where it can be noted that the H_V estimates presented greater values than the H_1 estimates, mainly close to the natural frequencies. These results showed to be a typical characteristic of both estimators, since it was observed for all experimental tests. The best results therefore were obtained when both estimates tended to similar values.

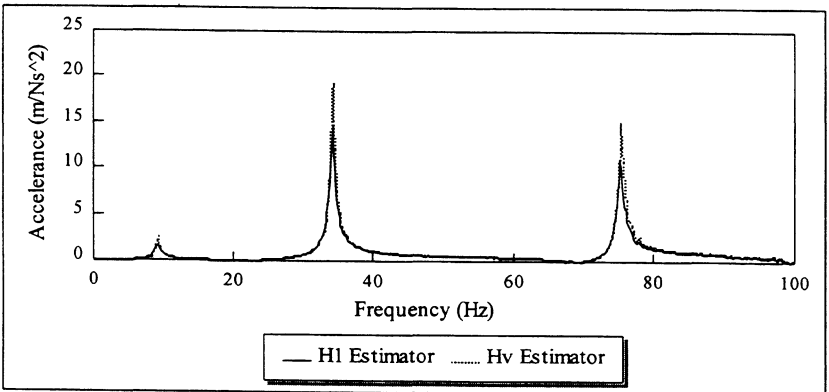

Figure 6 - Comparison of the Results Obtained for H_1 and H_V Estimators of the Accelerance for the Force in AC1 and the Response Measured in AC1.

Experimental tests were carried on the simply supported beam, in order to test the efficiency of the implemented system with multiple simultaneous input. Figure 7 shows the location of the input forces and the output responses. The input were random forces, and the correlation between both forces were never equal unity.

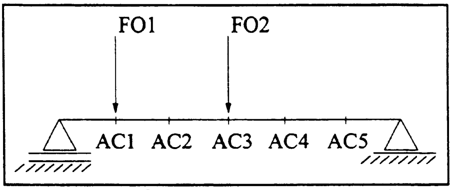

Figure 7 - Schematic Figure of the Simply Supported Beam Under Multiple Simultaneous Random Input Forces.

Figure 8 shows a comparison of the H_1 estimates obtained for the single random input force and for the multiple simultaneous random input forces. The results compare very well, showing the efficiency of the multiple simultaneous excitation implemented in the system.

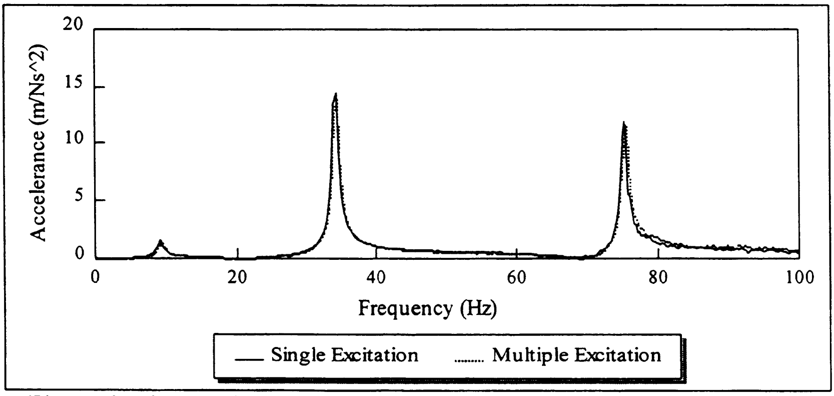

Figure 8 - Comparison of the Results for the H_1 Estimator Using Single Excitation and Multiple Simultaneous Excitation, for the Response Measured in AC1.

EXPERIMENTAL TESTS

Experimental tests were carried on a small scale model of an offshore platform for 100 meters water depth installed in Campos Basin[10]. Figure 9 shows a photo of the model, designed and constructed according to the similitude theory, with a geometric scale of 1/45. The model, built with PVC and ABS plastic tubes, was tested in order to evaluate the implemented system with complex structures and with a great number of sensors.

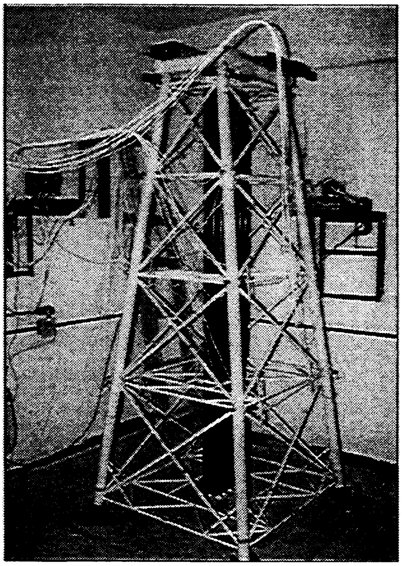

Figure 9 - Photo of the Small Scale Model of an Offshore Platform.

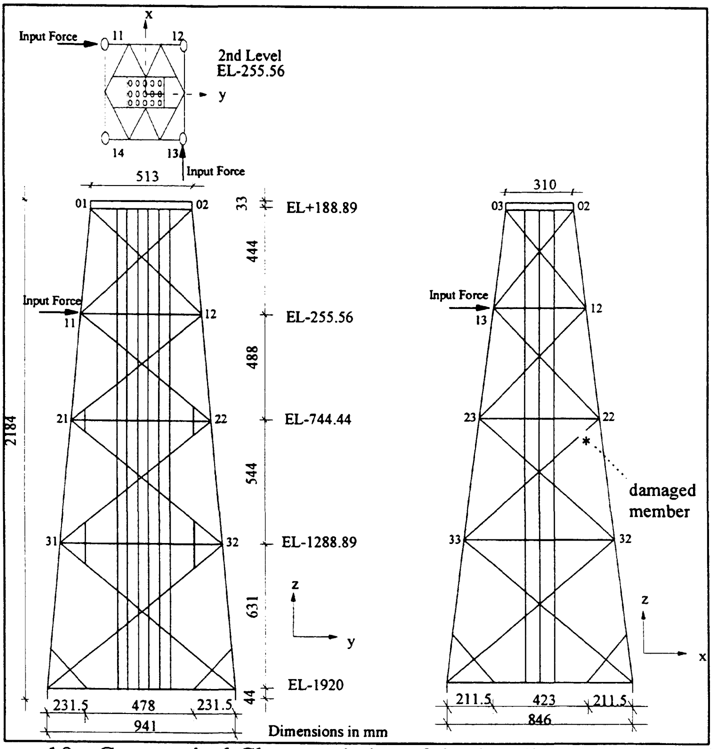

Figure 10 - Geometrical Characteristics of the Small Scale Model of an Offshore Platform.

The main geometric characteristics of the small scale model can be seen in Figure 10. The acceleration response was measured in 16 nodal points located in the main legs of the structure, in the x- and y-direction. Random forces were applied to the structure in x- and y directions, in order to excite the three first flexural and torsional modes in both directions.

Initially, tests were carried on to verify the linearity and the reciprocity of the platform. Figure 11 shows a comparison of the FRFs obtained for different levels of the force, applied in nodal point 13 in the x-direction (see Figure 10), and the response measured in nodal point 12 in the x-direction, where it can be noted the linearity of the structure. Figure 12 shows the FRFs obtained for the input force applied in nodal point 11 in y-direction and the response measured in nodal point 13 in x-direction compared with the FRF obtained for the input force applied in nodal point 13 in x-direction and the response measured in nodal point 11 in y-direction. The results compare very well, showing the reciprocity of the structure.

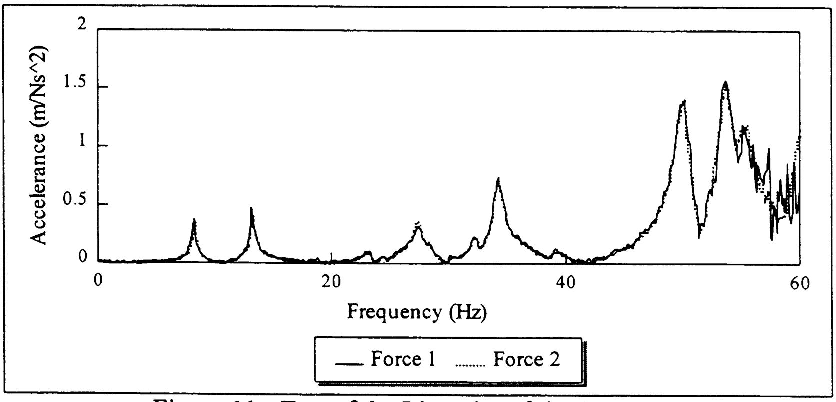

Figure 11 - Test of the Linearity of the Structure.

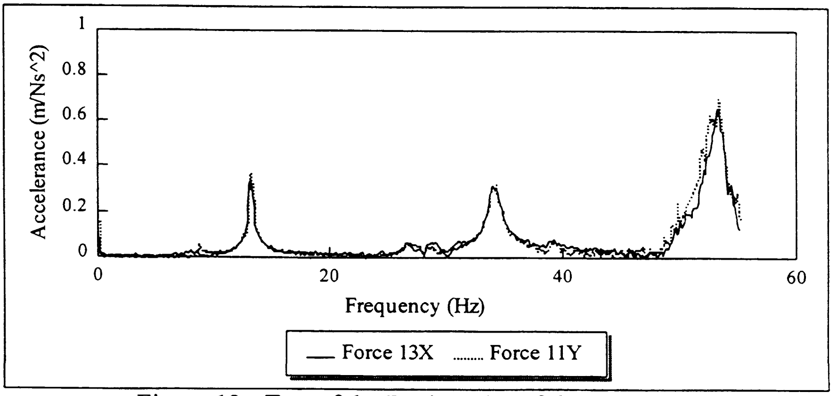

Figure 12 - Test of the Reciprocity of the Structure.

Experimental tests were carried on the structure for multiple simultaneous random input forces applied in nodal point 13 in the x-direction and in nodal point 11 in the y-direction. The 64 obtained FRFs for the 32 acceleration responses and the two simultaneous forces were used in a modal parameter estimation program, which uses the orthogonal polynomial method[5] for MIMO data. Table 1 shows the experimental modal parameters and the Figures 13-15 show the experimental mode shapes obtained using the parameter estimation program.

Table 1 - Experimental Modal Parameters of the Small Scale Model

Vibration Modes	Frequency (Hz)	Damping (%)
1st Flexural X	8.13	1.27
1st Flexural Y	8.58	1.37
1st Torsional	13.08	1.41
2nd Flexural X	27.02	2.83
2nd Flexural Y	29.14	1.25
2nd Torsional	34.03	1.42
3rd Flexural X	49.86	1.25
3rd Flexural Y	51.21	1.86
3rd Torsional	53.11	1.38

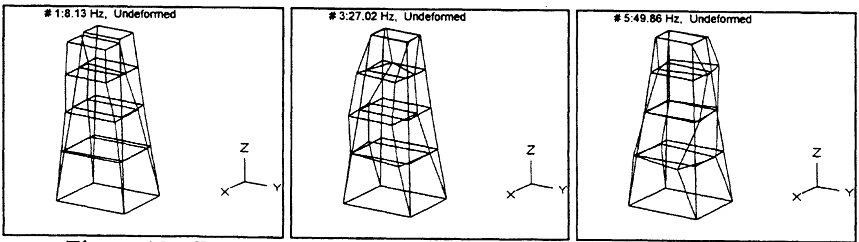

Figure 13 - Experimental Flexural Mode Shapes in the x-direction.

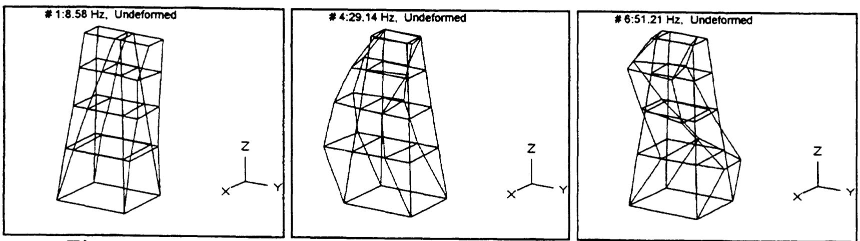

Figure 14 - Experimental Flexural Mode Shapes in the y-direction.

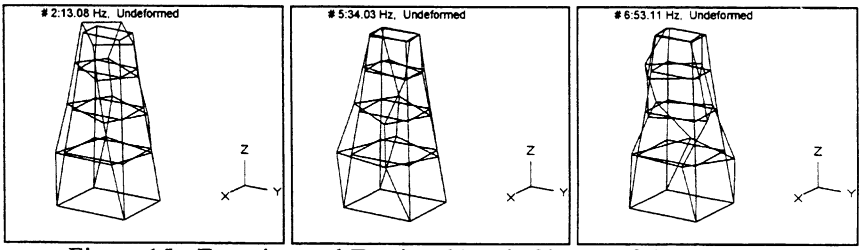

Figure 15 - Experimental Torsional Mode Shapes of the Structure.

In order to compare the mode shapes obtained with the single and multiple input forces, it was used the Modal Assurance Criterion[11] (MAC) correlation technique, which indicates the similitude between two sets of mode shapes. The main diagonal of the MAC matrix indicates how similar the two sets of mode shapes are: if they are close to unity (≥0.90)[12], they can be considered similar. The elements of the main diagonal of the MAC matrix showed in the first column of Table 2 showed the good correlation of the two sets of mode shapes, confirming once more the quality of the results obtained with the MIMO technique.

The MAC technique can also be used to identify the presence of damage in the structure. Damage was imposed to the structure by cutting the extremity of one of its diagonal member, as it can be seen in Figure 10, and the obtained mode shapes were compared with the mode shapes of the undamaged structure. The MAC values presented in the first column of Table 2 were taken as reference. The MAC values for the mode shapes of the undamaged and damaged structure are showed in the second column of Table 2. It can be observed that the results, mainly for the higher modes, were different from unity and from the values of the first column, indicating the occurrence of damage. Since the damage was imposed in a member in the x-direction of the structure, the results for the flexural modes in the x-direction and for the torsional modes showed a greater variation than for the flexural modes in the y-direction.

Table 2 - Main Diagonal of the MAC Matrix

Vibration Modes	Single Input x Multiple Input	Undamaged x Damaged
1st Flexural X	0.99	0.99
1st Flexural Y	1.00	1.00
1st Torsional	1.00	0.98
2nd Flexural X	0.99	0.87
2nd Flexural Y	1.00	0.99
2nd Torsional	1.00	0.93
3rd Flexural X	0.90	0.54
3rd Flexural Y	0.99	0.95
3rd Torsional	0.99	0.69

CONCLUSIONS

Analyzing the results of the experimental tests, the efficiency and accuracy of the implemented system for the estimation of FRFs using the MIMO technique was demonstrated. The LabVIEW platform showed to be suitable for the development of the system, not only for its graphical facilities, but also for the possibility of hardware upgrade, enabling the use of one hundred sensors simultaneously.

The implemented FRF estimators H_1 and H_V showed good accuracy, but it could not be demonstrated a major efficiency from one estimator over the other. The observed tendency of the estimators, that the H_1 estimates presented values a little lower than the H_V, could be used for a validation of the quality of the results, since the best results were observed when both estimates tended to be similar.

The use of multiple simultaneous excitation showed to be of great importance, since orthogonal modes could be excited in one experimental test, decreasing the errors due to environmental variations which occurs in offshore structures, like wave height, wind and sea current.

REFERENCES

[1] Allemang, R.J.; *Investigation of Some Multiple Input/Output Frequency Response Function Experimental Modal Analysis Techniques*, Ph.D. Dissertation, University of Cincinnati, 1980.

[2] Leuridan, J.M.; *Some Direct Parameter Model Identification Methods Applicable for Multiple Input Modal Analysis*, Ph.D. Dissertation, University of Cincinnati, 1984.

[3] Rost, R.W.; *Investigation of Multiple Input Frequency Response Function Estimation Techniques for Experimental Modal Analysis*, Ph.D. Dissertation, University of Cincinnati, 1985.

[4] Lembregts, F.; *Frequency Domain Identification Techniques for Experimental Multiple Input Modal Analysis*, Ph.D. Dissertation, Katholiek Universiteit Leuven, 1988.

[5] The STAR System User and Reference Manuals, 1994.

[6] Bendat, J.S. and Piersol, A.G.; *Random Data, Analysis and Measurements Procedures*, 2nd Edition, New York, Wiley-Interscience, 1986.

[7] Rost, R., Leuridan, J., "A Comparison of Least Squares and Total Least Squares for Multiple Input Estimation of Frequency Response Functions", *ASME paper nº 85-DET-105*, 6 pp, 1985.
[8] Rocklin, G.T., Crowley, J., Vold, H., "A Comparison of H_1, H_2 and H_V Frequency Response Functions", In: *Proceedings of the 3rd International Modal Analysis Conference*, pp.272-278, 1985.
[9] LabVIEW Manuals, Ver. 4.0, 1996.
[10] Viero, P.F., *Verification of the Influence of Structural Damages in the Modal Parameters of Fixed Offshore Structures*, M.Sc. Dissertation (in Portuguese), COPPE/UFRJ, 1991.
[11] Allemang, R.J., Brown, D.L., "A Correlation Coefficient for Modal Vector Analysis", In: *Proceedings of the 1st International Modal Analysis Conference*, pp.110-116, 1983.
[12] Ewins, D.J., *Modal Testing: Theory and Practice*, London, Research Studies Press Ltd., 1984